DYNAMIC SIGNAL STRENGTH MAPPING AND ANALYSIS BY MEANS OF MOBILE GEOGRAPHIC INFORMATION SYSTEM

Marcin Kulawiak, Witold Wycinka

Gdańsk University of Technology, Faculty of Electronics, Telecommunication and Informatics, G. Narutowicza 11/12, 80-233 Gdańsk, Poland (✉ Marcin.Kulawiak@eti.pg.edu.pl, +48 58 347 1728, Witek.Wycinka@wp.pl)

Abstract

Bluetooth beacons are becoming increasingly popular for various applications such as marketing or indoor navigation. However, designing a proper beacon installation requires knowledge of the possible sources of interference in the target environment. While theoretically beacon signal strength should decay linearly with log distance, on-site measurements usually reveal that noise from objects such as Wi-Fi networks operating in the vicinity significantly alters the expected signal range. The paper presents a novel mobile Geographic Information System for measurement, mapping and local as well as online storage of Bluetooth beacon signal strength in semi-real time. For the purpose of on-site geovisual analysis of the signal, the application integrates a dedicated interpolation algorithm optimized for low-power devices. The paper discusses the performance and quality of the mapping algorithms in several different test environments.

Keywords: beacon, mapping, GIS, geovisual analytics.

1. Introduction

Mapping signal strength constitutes an important issue in many challenges, related *e.g.* to indoor navigation [1]. Because of this, effective methods of mapping signal strength have been the subject of intense research for many years. Thus far, construction of signal strength maps has required the use of a complex measuring setup [2], with the collected results being processed using a dedicated desktop [3] or cloud-based software [4]. This has been primarily accomplished by the interpolation algorithms such as *Inverse Distance Weighting* (IDW) [5] and kriging [6] which have shown to produce accurate signal maps [7−10] at the cost of high computational complexity [11, 12]. Because of this, the processes of data collection, analysis and visualization have often been performed in separate hardware and software environments [13]. Moreover, on-site visualization of collected data has only been available using a laptop or a terminal device acting as a client for a cloud-based processing system [14]. However, recent developments in modern libraries dedicated to processing of geographical data have introduced the potential of collection, display and analysis of spatial data within a single instance of a *Geographic Information System* (GIS) [15, 16]. In addition, the successive advancements in the development of high-performance mobile devices has opened a pathway to the integration of data collection, storage, visualization and analysis on a single battery-powered device.

In-situ interpolation, mapping and analysis of signal strength data could quickly identify possible sources of interference and thus significantly improve *e.g.* the process of planning Bluetooth beacon placement for optimal area coverage. However, because the established data interpolation algorithms such as kriging and IDW are too computationally complex to use them on mobile devices, no such tools have been created thus far. In the above context, we propose a new mapping and analysis algorithm, optimized for use in real time on mobile devices and

designed in accordance to the paradigms of Geovisual Analytics. The algorithm has been implemented and tested as part of a novel mobile Geographic Information System for dynamic collection, mapping and analysis of Bluetooth beacon signal strength for the purpose of indoor applications. In the paper we compare the performance and interpolation quality of the proposed algorithm with those offered by IDW and kriging for the same datasets. The interpolation results are cross-validated with in-situ measurements, and the uncertainty of produced maps is discussed. Finally, we present details of the mobile GIS architecture and discuss the results of testing the system in three distinct indoor environments.

2. Materials and methods

Recently, more and more indoor services (including *e.g.* direct marketing or navigation) are provided using electronic beacons. A beacon broadcasts its unique identifier to nearby electronic devices using a standard protocol and frequency. The most commonly used electronic beacons employ the *Bluetooth Low Energy* (BLE) standard, which has been introduced in version 4.0 of the Bluetooth specification [17]. Because BLE-compliant devices are not meant to transmit large volumes of data, the protocol has instead been optimized to provide stable connections in a range of 5 m to 15 m at very low power requirements [18]. Single-mode devices which only support BLE are commonly referred to as beacons. Beacons may be used together with any dual-mode Bluetooth 4.0 compliant device, which includes most modern smartphones [19]. Beacons are characterized by several parameters, many of which can usually be modified to some extent by the user. These include the device's transmit rate and power, its *Universally Unique Identifier* (UUID) as well as the communication protocol. Depending on the device and its configuration, Bluetooth beacons may continuously operate even for a few years [20].

The currently available beacons can be configured to operate using a variety of protocols. The most popular ones are iBeacon (developed by Apple Inc.) and Eddystone (developed by Google Inc.). The iBeacon protocol is a multi-purpose tool based on Bluetooth low energy proximity sensing. The protocol supports detection of devices which come into proximity to a single beacon, as well as monitoring the events of devices entering specific regions defined by a network of beacons [21]. However, because iBeacon is a proprietary protocol, building a universal signal analysis solution requires the use of an open protocol such as Eddystone. [22]. The Eddystone protocol is also based on the BLE standard, however it is an open specification released under the Apache 2.0 license, which makes it a cross-platform one and free to use. Currently, Eddystone supports broadcasting several types of frame data, including [23]:

- Eddystone-UID which sends out a unique identifier of the beacon, allowing for its identification by compatible devices in its proximity;
- Eddystone-URL which transmits a web address;
- Eddystone-TLM which transmits a set of the beacon's parameters such as a battery level, temperature or humidity;
- Eddystone-EID which broadcasts a dynamically changing Beacon ID, useful for security applications.

Due to its openness and compatibility with a wide range of devices, Eddystone was selected as the protocol to be used during the presented research. As a source of signal for mapping, a selection of Bluetooth beacons implementing the Eddystone protocol was acquired. The beacons in question are shown in Fig. 1.

Fig. 1. Beacons used in the presented research
(from left: AprilBeacon 227A, AprilBeacon sensor 401, Kontakt.io Smart Beacon).

The detailed specifications of the beacons used in the presented research may be found in Appendix 1.

For the purpose of mobile measurement and analysis of beacon signal strength, a dedicated Geographic Information System has been designed and implemented. The system was run on a Bluetooth 4.1 compatible smartphone with 2 GB of RAM and a quad-core Snapdragon 810 processor working at a maximum frequency of 2 GHz under the control of Android 5.01 operating system. The detailed architecture of the GIS as well as the principles of its operation are presented in the following section.

2.1. System architecture and operation

Electromagnetic signals exist in a common geographical context with other physical phenomena. In computer science, physical phenomena of various nature are commonly integrated, processed and analysed with the use of Geographic Information Systems [24, 25]. Although data integration and analysis has thus far been constrained to GIS running on Desktop or Server-class computer systems, the recent advancements in both cross-platform GIS libraries and mobile computing device performance has enabled the construction of an innovative solution which integrates data collection, processing and analysis on a single low-power mobile device. The architecture of the presented solution is shown in Fig. 2.

The system is built using modern web-enabled technologies such as HTML5. This makes the system modules architecture-independent which enables their cross-platform deployment and reuse. Although the mobile application of the system is self-contained and provides whole necessary functionality directly on a mobile device, the system gives users the option of backing up their measurements on a remote server.

When installed on an Android device, the Mobile application enables the collection of signal power data from the device's Bluetooth radio. From the user's perspective, the process involves placing the device in one of the designated measurement points, which are displayed on the device's screen in the form of a grid overlaid on the map of the area. Points which have not yet been assigned any measurement values are presented on the map in red colour. The collected data are stored in the Signal buffer, where they are averaged over a user-selectable period of time (by default, the application averages 30 consecutive measurement results). The data averaged by the Signal buffer are then passed on to the Database management module. The Database management module pre-processes the collected data for storage in a database. The data may be stored in the Local database as well as server-side, where they are received by the Front controller module and passed through the Server database management module. Once the data have been stored in a database, they may be displayed by the User interface module. Both the Database management and User interface modules are implemented using the Open-Source Convertigo platform, which delivers a secured and scalable cross-platform mobile development middleware [26]. The Local database may be pre-populated with a map of the relevant area,

which may be used as reference during measurements. The map is displayed by the system's GIS module, which is also used to assign a geographical reference to the collected data. The module is built using the Open-Source OpenLayers library [27]. OpenLayers allows for the construction of interactive GIS applications for display and manipulation of vector and raster geospatial data, which can be obtained from local sources such as GML and GeoJSON files, or external ones through open protocols such as WMS and WFS. Aside from enabling the collection of measurements in a geographical context, the GIS module provides real-time interpolation and mapping of the measured signal strength with the application of Geovisual Analytics [28]. The Geovisual Analytics sub-module employs distance-weighted interpolation of the collected discrete measurement data into a continuous map which covers the entirety of the relevant area. Moreover, the Geovisual Analytics sub-module enables adaptive matching of the displayed interpolation's colour palette to the current range of signal strength. The interpolated signal strength map is presented to the end user overlaid on the map of the relevant area.
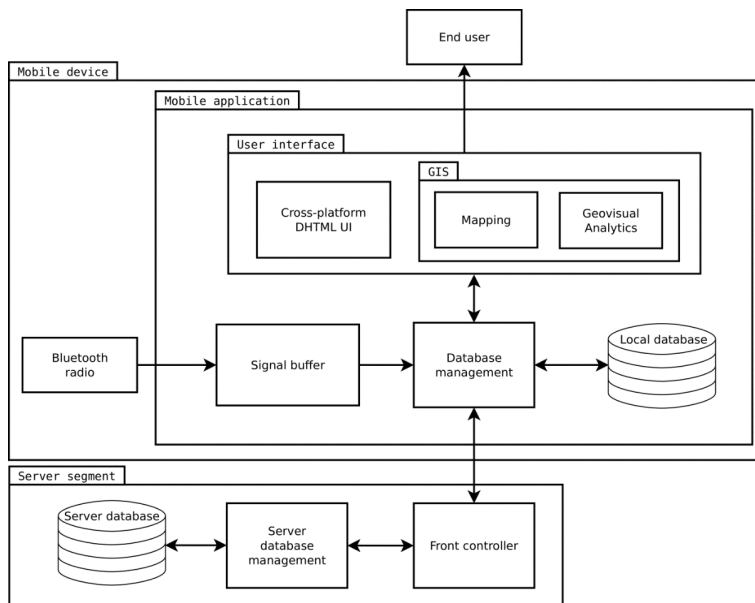

Fig. 2. Architecture of the system for mobile signal strength mapping and analysis.

2.2. Signal interpolation and mapping algorithm

Because the computational complexity of advanced interpolation algorithms such as IDW or kriging rises polynomially with the number of input points, computing high-resolution maps from a large number of measurements is not feasible on a mobile device. In response to this limitation, an optimized interpolation algorithm has been developed. The proposed algorithm assumes a regularized grid of input measurements which must be taken by the user. If a point cannot be measured (*e.g.* because of an obstacle), the value of signal at this point is interpolated using the closest known values in its horizontal and vertical neighbourhood on the grid. The final grid is then used to create a continuous map of the relevant area by interpolating values between neighbouring data points. The applied interpolation method, similarly to IDW and kriging, is derived from the Tobler Law [29] and uses distance weighting to estimate values for unmeasured locations. However, thanks to the grid generated in the first step of the algorithm,

the distances are only analysed in the local instead of global context, which brings significant time savings. In particular, the value of the proposed interpolation function for a point (x, y) is given by the formula:

$$f(x,y) = \sum_{i=1}^{N} w_i(x,y) f(x_i, y_i),$$ (1)

where: $N \in (1; 4)$ is a number of analysed neighbouring measurement points; $f(x_i,y_i)$ is a signal value measured at point i and $w_i(x,y)$ is a weight of the i-th neighbouring measurement point, as per the uniform weight function:

$$w_i(x,y) = e^{\left(-\left(\frac{x-x_i}{dx}\right)^2 - \left(\frac{y-y_i}{dy}\right)^2\right)}.$$ (2)

In the above formula, a point (x_i, y_i) denotes the location of the i-th measured value and dx, dy are the x and y distances between adjacent measurement points in the grid.

The performance of the proposed interpolation algorithm has been tested on a mobile device equipped with 2 GB of RAM and a Qualcomm Snapdragon 810 quad-core CPU working with a maximum frequency of 2.0 GHz. The tests measured time required for computation and rendering of a 1080×1100 pixel signal map interpolated from 165 measurement points from the Large Hall dataset (which is described in detail in Subsection 3.3). The performance was averaged over ten consecutive runs. As reference, the same dataset has been interpolated on the same device using javascript IDW implementation by Manuel Bär [30]. On average, the presented algorithm rendered the complete signal map in 531 ms, which means that a new interpolation is ready in less than a second after making a new measurement. For comparison, the IDW interpolation of the same dataset took on average 7302 ms. This difference is particularly significant because IDW is known to be one of the less computationally intensive interpolation methods, especially in comparison with kriging [31, 32].

The algorithm also compares favourably with other methods when it comes to interpolation quality. Fig. 3 presents a comparison of signal maps produced from the same dataset (the Small Flat dataset, described in detail in Subsection 3.3) by the proposed method as well as by the much more computationally complex IDW and Empirical Bayesian Kriging ones.
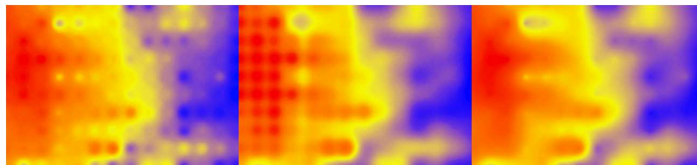

Fig. 3. Interpolations of the same set of measurements by IDW (left),
the proposed method (centre) and kriging (right).

As it can be observed in Fig. 3, the proposed method delivers a smooth interpolation which retains local details, very much like kriging. IDW on the other hand overly emphasizes the individual measurements, which results in a grid-like pattern on the interpolated map. In comparison with the proposed method, kriging predicts slightly lower signal strength values near the beacon (the area to the left shown in red colour), while IDW predicts a lower signal strength value in the centre of the flat area (shown in shades of orange and yellow). At the same time, the differences between values interpolated by kriging and IDW may be found in every part of the flat area, however their average values are very similar. Computing the mean absolute deviation between the values of each map produces a relative uncertainty of 19% between the proposed method and kriging, 31% between the proposed method and IDW, and 19% between kriging and IDW.

The assessment of relative interpolation quality of the proposed method requires cross-validation of the interpolated values with in-situ measurements. For this purpose, the Small Flat dataset has been divided in two. A regular subset representing approximately 14% of all points, selected from every second row and column has been removed, and the remaining dataset has been used to perform interpolation using the proposed method as well as kriging and IDW. The smaller data subset was then used to sample the resulting rasters in the exact locations of the original measurements. Computing the mean absolute deviation between the original measurements and values predicted by each method produces a relative uncertainty of 31% for kriging, 35% for the proposed method and 50% for IDW.

According to the Bluetooth specification, a signal recorded by a Bluetooth radio has a relative value uncertainty of 6% to 10% depending on the device [17, 33]. Assuming an average relative measurement uncertainty of 0.7% and the use of a low quality Bluetooth receiver, the signal maps produced by the presented system have a relative combined standard uncertainty of $(0.19^2 + 0.35^2 + 0.1^2 + 0.007^2)^{(1/2)} = 41\%$. This is a very good result, considering the fact that if the same maps could be created on a mobile device by means of more advanced methods, their relative combined standard uncertainty would be 38% for kriging and 55% for IDW.

As it can be seen, the initial research suggests that the proposed algorithm produces signal strength maps with a quality similar to the computationally-intensive kriging, while providing a significantly better performance on a mobile device than even the less computationally complex IDW.

In the above context, the developed system has been tested in several different environments. The results of those tests are presented in the following section.

3. Results and discussion

Mapping signal strength indoors requires a reliable and appropriately powerful source. Because of this, it was necessary to test and compare characteristics of the three Bluetooth beacons in an open environment. First, every beacon was put in its maximum transmission power mode (where possible). Then, one after another, the beacons were placed on an elevated surface in an interference-free area and their signal decay characteristics were measured in one-metre distances (every recorded value was averaged from 50 consecutive measurements). Finally, the results were analysed using the application's measurement plot feature. The average relative uncertainty of the measurements was approximately 0.7%. The results may be found in Fig. 4.
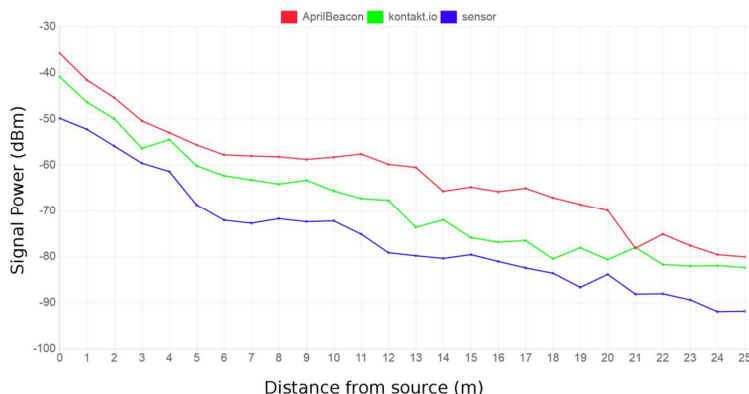

Fig. 4. Signal decay characteristics of the examined Beacons.

www.czasopisma.pan.pl   www.journals.pan.pl

Metrol. Meas. Syst., Vol. 24 (2017), No. 4, pp. 595–606.

As it can be seen in Fig. 4, AprilBeacon 227A in its strongest configuration (signal power of 4 dBm) provided the best signal quality in an open environment, with the signal being readable even 25 m from the source. Despite the same power configuration (4 dBm), the signal produced by Kontakt.io was on average 6 dBm lower than AprilBeacon 227A. This may be attributed to the latter's lack of an external antenna. The AprilBeacon sensor 401 provided the lowest signal power, on average 7 dBm weaker than Kontakt.io. Basing on the above results, it was decided that AprilBeacon 227A in its strongest configuration would be used for further measurements.

Once the source of the signal was selected, the presented system has been applied to mapping and analysis of BLE signal strength in three different environments. The obtained results may be found below.

3.1. Test environment 1: Empty Hallway

The first test environment was an empty hallway with four closed wooden doors in the side walls. The walls are made of 12 cm-thick bricks. The main entrance to the hallway is through a glass door in the back. The wall opposite the main entrance has a line of glass windows. The floor is covered with lacquered rubber boards, while the suspended ceiling is made of drywall. The source beacon was placed to the right of the main entrance, approximately 1.2 m above the floor. Fig. 5 presents the recorded Beacon signal strength map for this environment (the position of the beacon is marked with x). The measurements were performed in 1 m intervals, and every recorded value was averaged from 50 consecutive measurements. The average relative uncertainty of the measurements was 0.7%.
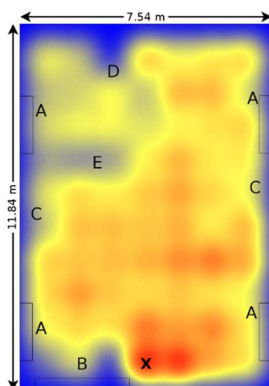

Fig. 5. A beacon signal strength map for the Empty Hallway. Red colour denotes the highest recorded signal power (−59,2 dBm), while the lowest recognizable signal (−93,3 dBm) is represented with blue colour.

The analysis of the signal strength map generated by the system shows some typical wave phenomena in the analysed environment. First of all, it is possible to observe a sharp drop in signal strength caused by the absorption of the signal through the wooden door on both sides of the hallway (points A). In those places a large part of the signal is radiated onto the outside corridors. A similar situation occurs at point B, where the signal is absorbed by the main entrance of the hallway. Interference was also likely caused by metal benches located near both side walls (points C) as well as a Wi-Fi router on the ceiling (point D). Further analysis revealed a decline in the signal strength at point E, which may be attributed to the interference caused by a Wi-Fi router on the lower floor.

3.2. Test environment 2: Large Hall

The second test environment was a large hall with walls made of 30 cm-thick breezeblocks. The hall has two sets of wooden door with glass windows on opposite side walls. There are four concrete pillars in the hall, two near each of the side walls. The floor is covered with carpeted felt. The beacon was placed near the middle of the hall approximately 1.8 m above the floor. Fig. 6 presents the recorded Beacon signal strength map for this environment (the position of the beacon is marked with x). The measurements were performed in 1 m intervals and every recorded value was averaged from 50 consecutive measurements. The average relative uncertainty of the measurements was 0.7%.
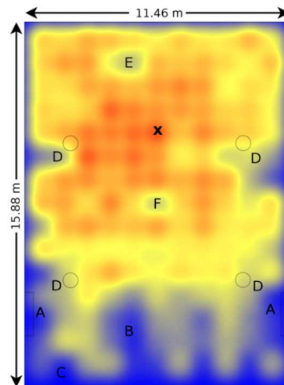

Fig. 6. A beacon signal strength map for the Large Hall. Red colour denotes the highest recorded signal power (−63,3 dBm), while the lowest recognizable signal (−93,1 dBm) is represented with blue colour.

Some of the typical phenomena observed in the previous test environment may be seen here as well. This includes signal anomalies near the wooden doors (points A) as well as interference form Wi-Fi routers inside the hall (points B and C). Aside from those, it is also possible to discern signal occlusion caused by the four concrete pillars (points D). Moreover, it is easy to spot a general loss of signal strength in the area of the concrete pillars, which is likely due to scattering caused by the round shape and smooth surface of the pillars. Further analysis attributed the decline in the signal strength in points E and F to the interference caused by Wi-Fi routers located on the upper floor.

3.3. Test environment 3: Small Flat

The final test environment was a flat in a five-storey building. The flat features load-bearing walls made of 35cm-thick concrete blocks and partition walls made of 12 cm-thick bricks. Ceilings are built of reinforced concrete with a thickness of 20 cm. The floor is covered with lacquered boards. The study area consists of a hallway, an office room with pieces of furniture such as desks, a kitchen and one room with plenty of free space. In order to minimize the impact of floor-level obstacles on the Fresnel zone, the beacon was mounted near the middle of the leftmost apartment wall at a height of 2.30 m. Fig. 7 presents the recorded Beacon signal strength map for this environment (the position of the beacon is marked with x). Because this space was considerably more tightly-packed than the previous ones, the measurements here were performed in 0.5 m intervals and every recorded value was averaged from 50 consecutive measurements. The average relative uncertainty of the measurements was approximately 0.75%.
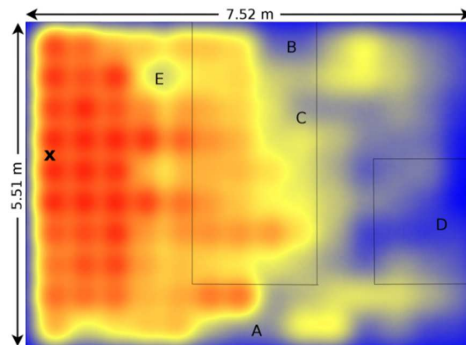
Fig. 7. A beacon signal strength map the Small Flat. Red colour denotes the highest recorded signal power (–44,3 dBm), while the lowest recognizable signal (–94,5 dBm) is represented with blue colour.

The signal map presented in Fig. 7 enables one to easily identify potential sources of interference and assess their impact on the recorded signal strength. A sharp decrease in signal power is evident in point A, where a Wi-Fi router using the 2.4 GHz band was placed. A similar situation may be observed in point B, where a Wi-Fi client computer was located. Moreover, signal-shielding metal objects (such as a large wall-mounted heater) were situated in the vicinity of measurement point C. Similarly, kitchen appliances such as an oven and a dishwasher are responsible for noticeable decreases in the recorded signal power for point D. Further analysis revealed that the sharp drop in the signal power in point E was caused by a Wi-Fi router located on the floor below. Analysis of the signal strength map of the entire apartment reveals a significant decline in strength of the signal passing through the brick walls of the room in the middle. Moreover, a decrease in the recorded signal power was even greater behind walls covered with ceramic tiles, such as those in the kitchen (around point D).

4. Summary

The paper presents the development and first field tests of an innovative mobile Geographic Information System for Bluetooth beacon signal mapping. Testing the system in several different environments has proved that it is capable of providing on-site signal strength interpolation and mapping in real time on a plain smartphone with Android OS. Moreover, the applied dedicated interpolation algorithm has shown to produce relatively high quality results, comparable to those offered by kriging, and better than those provided by IDW (both of them being much more computationally complex interpolation methods). This being said, it should be noted that the applied mobile optimizations require the algorithm to work with a regularized measurement grid and thus should not be applied to the interpolation of sparse irregular measurements (which in turn are known to be handled properly by both kriging and IDW). Still, the applied optimizations enable the system to work in semi-real time, producing signal strength maps directly on a mobile device during measurements. Moreover, the system applies Geovisual Analytics for adaptive signal strength colour palette matching, which ensures good visibility of local signal power spikes and enables easy identification of possible sources of interference. The interpolated signal strength map is presented to the end user overlaid on the map of the relevant area.

The presented results indicate that features like real-time signal measurement, interpolation and analytical mapping, coupled with cloud backup capabilities, make the system a flexible tool for researchers as well as engineers working on indoor beacon applications such as proximity sensing and navigation.

References

[1] Liu, S., Chen, Y., Trappe, W., Greenstein, L.J. (2009). Non-interactive localization of cognitive radios based on dynamic signal strength mapping. *2009 Sixth International Conference on Wireless On-Demand Network Systems and Services*, Snowbird, UT, 85–92.

[2] Yin, J., Yang, Q., Ni, L.M. (2008). Learning adaptive temporal radio maps for signal-strength-based location estimation. *IEEE Transactions on Mobile Computing*, 7(7), 869–883.

[3] Ji, Y., Biaz, S., Pandey, S., Agrawal, P. (2006). ARIADNE: a dynamic indoor signal map construction and localization system. *Proc. of the 4th international conference on Mobile systems, applications and services,* 151–164.

[4] de Moraes, L.F.M., Nunes, B.A.A. (2006). Calibration-free WLAN location system based on dynamic mapping of signal strength. *Proc. of the 4th ACM international workshop on Mobility management and wireless access*, 92–99.

[5] Shepard, D. (1968). A two-dimensional interpolation function for irregularly-spaced data. *Proc. of the 1968 23rd ACM national conference*, 517–524.

[6] Matheron, G. (1963). Principles of geostatistics. *Economic Geology*, 58(8), 1246–1266.

[7] Connelly, K., Liu, Y., Bulwinkle, D., Miller, A., Bobbitt, I. (2005). A toolkit for automatically constructing outdoor radio maps. *International Conference on Information Technology: Coding and Computing (ITCC'05)-Volume II*, 248–253.

[8] Phillips, C., Ton, M., Sicker, D., Grunwald, D. (2012). Practical radio environment mapping with geostatistics. *2012 IEEE International Symposium on Dynamic Spectrum Access Networks*, Bellevue, WA, 422–433.

[9] Wielgosz, P., Grejner-Brzezinska, D., Kashani, I. (2003). Regional ionosphere mapping with kriging and multiquadric methods. *Journal of Global Positioning Systems*, 1(4), 48–55.

[10] Lee, H. K., Li, B., Rizos, C. (2005). Implementation procedure of wireless signal map matching for location-based services. *Proc. of the Fifth IEEE International Symposium on Signal Processing and Information Technology*, 429–434.

[11] Kerry, K.E., Hawick, K.A. (1998). Kriging interpolation on high-performance computers. *International Conference on High-Performance Computing and Networking*, 429–438.

[12] Murphy, R.R., Curriero, F.C., Ball, W.P. (2009). Comparison of spatial interpolation methods for water quality evaluation in the Chesapeake Bay. *Journal of Environmental Engineering*, 136(2), 160–171.

[13] Ye, S.J., Zhu, D.H., Yao, X.C., Zhang, X., Li, L. (2016). Developing a mobile GIS-based component to collect field data. *2016 Fifth International Conference on Agro-Geoinformatics (Agro-Geoinformatics)*, Tianjin, 1–6.

[14] Han, W., Hu, Y., Zhang, J., Liu, Q. (2015). Mobile Data Acquisition and Management System Design Based on GIS and GPRS. *Metallurgical and Mining Industry*, 2, 243–249.

[15] Moszynski, M., Kulawiak, M., Chybicki, A., Bruniecki, K., Bieliński, T., Łubniewski, Z., Stepnowski, A. (2015). Innovative Web-Based Geographic Information System for Municipal Areas and Coastal Zone Security and Threat Monitoring Using EO Satellite Data. *Marine Geodesy*, 38(3), 203–224.

[16] Kulawiak, M., Kulawiak, M. (2017). Application of Web-GIS for Dissemination and 3D Visualization of Large-Volume LiDAR Data. *The Rise of Big Spatial Data*, Springer International Publishing, 1–12.

[17] Bluetooth Special Interest Group. Specification of the Bluetooth® System, version 4.2. 2014. *https://www.bluetooth.org/DocMan/handlers/DownloadDoc.ashx?doc_id=286439* (Nov. 2016).

[18] Gomez, C., Oller, J., Paradells, J. (2012). Overview and evaluation of Bluetooth low energy: An emerging low-power wireless technology. *Sensors*, 12(9), 11734–11753.

[19] Townsend, K., Cufí, C., Davidson, R. (2014). *Getting started with Bluetooth low energy: tools and techniques for low-power networking*. O'Reilly Media, Inc.

[20] Mackensen, E., Lai, M., Wendt, T.M. (2012). Performance analysis of an Bluetooth Low Energy sensor system. *2012 IEEE 1st International Symposium on Wireless Systems (IDAACS-SWS)*, Offenburg, 62–66.

www.czasopisma.pan.pl   PAN   www.journals.pan.pl
POLSKA AKADEMIA NAUK

Metrol. Meas. Syst., Vol. 24 (2017), No. 4, pp. 595–606.

[21] Getting Started with iBeacon. (2014). Apple Inc. *https://developer.apple.com/ibeacon/Getting-Started-with-iBeacon.pdf* (Nov. 2016).

[22] iBeacon – Frequently Asked Questions. (2014). Cisco Inc. *http://www.cisco.com/c/dam/en/us/solutions/collateral/enterprise-networks/connected-mobile-experiences/ibeacon_faq.pdf* (Nov. 2016).

[23] Eddystone protocol specification. (2016). *https://github.com/google/eddystone/blob/master/protocol-specification.md* (Nov. 2016).

[24] Moszynski, M., Chybicki, A., Kulawiak, M., Lubniewski, Z. (2013). A novel method for archiving multibeam sonar data with emphasis on efficient record size reduction and storage. *Polish Maritime Research*, 20(1), 77–86.

[25] Kulawiak, M. (2016). Operational algae bloom detection in the Baltic Sea using GIS and AVHRR data. *Baltica*, 29(1), 3–18.

[26] *www.convertigo.com* (Apr. 2017).

[27] *openlayers.org* (Apr. 2017).

[28] Andrienko, G., Andrienko, N., Jankowski, P., Keim, D., Kraak, M. J., MacEachren, A., Wrobel, S. (2007). Geovisual analytics for spatial decision support: Setting the research agenda. *International Journal of Geographical Information Science*, 21(8), 839–857.

[29] Tobler, W. (1970) A computer movie simulating urban growth in the Detroit region. *Economic Geography*, 46(2), pp. 234–240.

[30] Bär, M. *www.geonet.ch* (Apr. 2017).

[31] Reed, P.M., Ellsworth, T.R., Minsker, B.S. (2004). Spatial interpolation methods for nonstationary plume data. *Ground Water*, 42(2), 190–202.

[32] Murphy, R.R., Curriero, F.C., Ball, W.P. (2009). Comparison of spatial interpolation methods for water quality evaluation in the Chesapeake Bay. *Journal of Environmental Engineering*, 136(2), 160–171.

[33] Bluetooth Special Interest Group. Specification of the Bluetooth® System, version 1.0. 1999. *http://ece.wpi.edu/analog/resources/bluetooth_a.pdf* (Nov. 2016).

Appendix 1: Detailed specifications of used Bluetooth beacons

Table 1. Specifications of Kontakt.io Smart Beacon.

Parameter	Value
Transmission Power	−30 dBm to 4 dBm
Sensitivity	−93 dBm
Working temperature	−20ºC to +60ºC
Processor	32-bit Arm Cortex MO CPU core
Bluetooth processor	Nordic nRF51822
Data rate	250 kb/s to 2 Mb/s
Flash memory size	256 kB
Ram size	16 kB
Battery	1x 1000 mAh CR2477
Exchangeable battery	yes
Battery life at 350 ms broadcast interval	2 years
External antenna	no
Minimum number of units sold	3
Price per unit	27 $

Table 2. Specifications of AprilBeacon 227A.

Parameter	Value
Transmission Power	−23 dBm to 4 dBm
Working temperature	−40ºC to +85ºC
Processor	Texas instruments 8051
Bluetooth processor	Texas instruments CC2540
Data rate	250 kb/s to 2 Mb/s
Flash memory size	256 kB
Battery	2x AAA (1000 mAh)
Exchangeable battery	yes
Battery life at 100 ms broadcast interval	4,5 month
External antenna	yes, 50 Ω
Price per unit	12 $

Table 3. Specifications of AprilBeacon sensor 401.

Parameter	Value
Working temperature	−40ºC to +85ºC
Processor	Texas instruments 8051
Bluetooth processor	Texas instruments CC2541
Data rate	250 kb/s to 2 Mb/s
Flash memory size	256 kB
Ram size	8 kB
Battery	1x 620 mAh CR2450
Exchangeable battery	yes
Battery life at 100 ms broadcast interval	2 months
Sensors	Light sensor, accelerometer, vibration sensor
External antenna	no
Price per unit	22 $